Calculation of Critical Load for Pure Distortional Buckling of Lipped Channel Columns

Imene Mahi[1]*, Mohamed Djelil[2], Naoual Djafour[2], Mustapha Djafour[2]

[1] Department of Civil Engineering, Faculty of Technology, EOLE Laboratory, University of Tlemcen, B.P. 230, Tlemcen 13000, Algeria
[2] Department of Civil Engineering, Faculty of Technology, RISAM Laboratory, University of Tlemcen, B.P. 230, Tlemcen 13000, Algeria
* Corresponding author, e-mail: imenemahi@gmail.com

Abstract

This paper presents a method that allows calculating the elastic critical stress for the distortional buckling mode, based on the buckling mode classification of typical lipped channel columns. In our case, Cold-Formed Steel Lipped Channel Columns are subjected to compression. Moreover, in order to consolidate the important findings of this work, a comparative study was carried out to assess the reliability of various distortional buckling models that are provided by different design Standards. It was found that the American and Australian approaches, given in the codes of practice, are closer to the Finite Strip Method than to the European method. An analytical solution was proposed for the determination of the distortional buckling stress on the basis of a statistical method; it corresponds to lipped channel sections with a flange width to web width ratio b/h ranging from 0.1 to 1, and a lip width to web width ratio c/h between 0 and 0.5. After comparison with the results given by the finite strip method for pure distortional buckling, it turned out that the proposed approach provides a reasonable prediction for the elastic distortional buckling stress for lipped channel sections subjected to compression. In fact, this method gives better results than the American approach.

Keywords

distortional buckling, lipped channel, analytical solution, compression, finite strip method

1 Introduction

Over the last decade, cold-formed steel members have increasingly been used as load-bearing and non-load-bearing elements. They have undergone significant development and are actually used in low-rise and mid-rise residential buildings as well as in non-residential constructions. It is worth noting that huge quantities of steel are currently employed in constructions. Indeed, large amounts of steel products can be shaped by cold-working. In addition, the significant growth in the steel market share is mainly due to metal recycling, and also to the high strength of steel, its ease of use in constructions and also to its ability to protect buildings in the event of an earthquake. However, using cold formed weathering steels may lead to members with high width/thickness ratios.

When cold-formed members are subjected to compression, they require appropriate and special consideration. In most cases, these members exhibit complex behavior that is essentially governed by local, distortional and global stability phenomena as well as their potential interactions.

The local buckling assumes that the junction lines between the intersecting planes remain straight and the cross-sectional shape of members undergoes distortion.

This buckling phenomenon induces a strength reduction due to the shift in the effective center of mass of the section. In addition, the buckling length may also be less than the largest dimension that characterizes the element. Moreover, the distortional buckling, which represents a failure mode for compressed or bended thin-walled sections, occurs at an intermediate half-wavelength of the buckling. The deformation of the section in this distortional mode is characterized by the rotation and translation of the edge-stiffened flange about the web-flange junction, as illustrated in Fig. 1. This phenomenon is generally engendered by buckling of the compressed flange-lip component [1].

For Euler buckling, at relatively long wavelengths, the entire section translates or rotates without significant changes in the cross-sectional shape. It is well known that thin-walled members exhibit a significant post-buckling
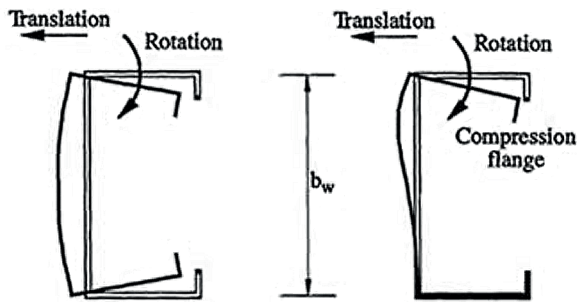
Fig. 1 Distortional buckling mode for a steel member subjected to compression and bending [24]

reserve for local buckling, but not for global buckling [2]. In addition, numerical and experimental analyses suggest that the distortional post-buckling behavior is stable; and distortional failures have higher imperfection sensitivity [3].

In fact, a reliable method for computing the *elastic critical moment* or *load* of the three basic buckling modes plays a crucial role in assessing the load-carrying capacity of thin-walled structural members. Analytical formulas or numerical methods, such as the finite element method [4–5] or finite strip method [6–7], may be used to perform an accurate evaluation of the *elastic critical moment* (*load*). Moreover, analytical expressions for the evaluation of the elastic local and Euler buckling stresses are available in Timoshenko and Gere [8], whereas the distortional buckling prediction can usually be based on *an analytical model* of *flange-lip combination* with rotational and translational stiffness at the junction point [9]. Furthermore, a great number of studies provide explicit formulae for predicting the critical distortional buckling stress. Several analytical models are available for columns [10–11], beams [12] and beam-columns [13]. In [14], a novel strength design curve, based on Hancock's curve, is proposed for predicting the load-carrying capacity in the distortional mode. Furthermore, the distortional buckling models that are available in the current design standards are quite complex and are difficult to use; models founded on straightforward intuition are needed. Therefore, a simpler and more practical solution for distortional mode is required to help engineers and researchers in designing, in an efficient way, the distortional buckling of cold-formed steel sections.

The present study aims to provide an analysis method for the calculation of pure distortional buckling stress based on a buckling mode classification of cold-formed steel (CFS) sections while considering the local buckling behavior. The interaction between the internal elements forming the compressed cross-section is adequately taken into consideration.

Very careful observation reveals the presence of eight zones that govern the behavior of lipped channel sections with a flange width to web width ratio (b/h) ranging from 0.1 to 1, and a lip width to web width ratio between 0 and 0.5. On the other hand, a comparative study was conducted on the analytical approaches (models) that are currently employed in common Design Standards of cold-formed steel structural members, such as AISI/NAS S100 (2007) [16], AS/NZS4600 (2005) [17], and CEN/EC3 EN 1993-1-3 (2006) [18]. Furthermore, a numerical analysis based on the finite strip method (FSM) was conducted for the purpose of evaluating the distortional buckling behavior under compression. This analysis was performed on a series of high strength steel lipped channel columns. The results obtained suggest that the findings given by the American model are consistent with those of the finite strip method in all zones, except in 1 and 5. The results corresponding to these zones could be improved using the new approach which provides better accuracy than the American design method.

2 Current formulas for elastic distortional buckling stress prediction
2.1 Generalities
The classical procedure for the evaluation of the strength of a structural member depends on the determination of the elastic critical load, which must then be corrected in order to consider the unfavorable effects of the different geometrical and material imperfections as well as the favorable effects of the post-critical strength reserve [20]. This correction is often performed with the help of the strength curves representing the evolution of elastic critical load and the ultimate load as a function of slenderness. This approach is adopted in most modern Design Codes such as CEN/EC3 EN 1993-1-3 (2006) [18], AS/NZS 4600 (2005) [17], and AISI/NAS S100 (2007) [16]. In this section, a brief overview of the existing analytical models for distortional buckling is provided. Moreover, the main governing formulae are also highlighted.

2.2 Current Design Standards AS/NZS 4600 (2005) and AISI/NAS S100 (2007) for distortional buckling
The approach adopted in the Australian/New Zealander Design Code (AS/NZS 4600, 2005) [17] indicates that distortional buckling involves mainly the rotation of the flange-lip combination as a rigid body about a web-flange junction. In this case, the contribution of the web is modeled by elastic springs that limit the deformation of the flange-lip subset, as illustrated in Fig. 2.
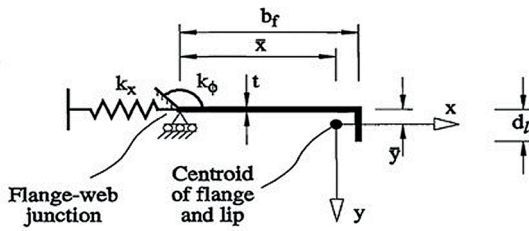
Fig. 2 Analytical model for distortional buckling of lipped flange [21]

The Lau and Hancock model [21] suggests that the translational spring stiffness can be assumed to be zero, and the rotational stiffness can be rewritten as Eq. (1):

$$k_\phi = \frac{Et^3}{5.46(h+0.06\lambda)}\left[1 - \frac{1.11 f'_{od}}{Et^2}\left(\frac{h^2\lambda}{h^2+\lambda^2}\right)\right]. \qquad (1)$$

Where f'_{od} is the elastic distortional buckling stress; it is calculated by assuming k_ϕ equal to zero, with λ as the buckling half-wavelength.

$$\lambda = 4.8\left(\frac{I_{xf} b^2 h}{t^3}\right)^{1/4} \qquad (2)$$

Also, I_{xf} is the moment of inertia of the flange along the x axis.

The distortional buckling stress can therefore be found as Eq. (3):

$$f_{od} = \frac{E}{2.A}\left\{(\alpha_1 + \alpha_2) - \sqrt{\left[(\alpha_1+\alpha_2)^2 - 4\alpha_3\right]}\right\}, \qquad (3)$$

where A is the cross-sectional area of the flange and the stiffener. $\alpha 1$, $\alpha 2$, and $\alpha 3$ are characteristic values which are given in sections D1 and D2 in Appendix D of Standard AS/NZS4500 (2005) [17].

The North American Specification for the Design of Cold-Formed Steel Structural Members [16] gives the following guidelines for evaluating the elastic distortional buckling stress:

The critical buckling length in which the distortional buckling occurs can be expressed as Eq. (4):

$$L_{cr} = \left(\frac{6\pi^4 h(1-v^2)}{t^3}\left(I_{xf}(x_o - h_x)^2 + C_{wf} - \frac{I_{xyf}^2}{I_{yf}}(x_o - h_x)^2\right)\right)^{1/4}. \qquad (4)$$

Where:

v = Poisson's ratio

x_o = distance x separating the flange/web junction from the centroid of the flange

h_x = distance x from the centroid of the flange to shear center of the flange

C_{wf} = warping torsion constant of the flange

I_{xyf} = Product of inertia of the flange

I_{yf} = y-axis moment of inertia of the flange

As for the elastic distortional buckling stress, it is expressed as Eq. (5):

$$f_d = \frac{K_{\phi fe} + K_{\phi we} + K_\phi}{\tilde{K}_{\phi fg} + \tilde{K}_{\phi wg}}. \qquad (5)$$

With:

$K_{\phi fe}$ = elastic rotational stiffness provided by the flange in the flange/web junction

$K_{\phi we}$ = elastic rotational stiffness provided by the web in the flange/web junction

K_ϕ = rotational stiffness at the flange/web junction of a member

$\tilde{K}_{\phi fg}$ = geometric rotational stiffness demanded by the flange at the flange/web junction

$\tilde{K}_{\phi wg}$ = geometric rotational stiffness demanded by the web at the flange/web junction

Schafer's definition given in the North American Specification [16] and that of Hancock of the Australian Standard are conceptually similar regarding the flange. However, Schafer's method gives an explicit treatment to the role of the elastic and geometric rotational stiffness at the web-flange junction. This quantity was introduced in the estimation of the critical elastic distortional stress. At this level, this method can account for the case where the buckling initially occurs as a result of web instability. The analytical model developed by the previous authors is based on the assumption that the behavior is governed by the flexural-torsional buckling of the flange-stiffener subset.

2.3 Current CEN/EC3 EN 1993-1-3 (2006) Standard for distortional buckling

The effective width concept initially developed by Von Karman et al., and was afterwards modified by Winter, is the main design procedure adopted in Eurocode 3 without any other alternatives [18]. This design method has been widely used in engineering practice for the computation of ultimate strength of slender members. Many design codes use this concept as a primary design approach in order to compensate the stiffness reduction in the post buckling; nonetheless, the effective width method does not provide an explicit procedure for predicting the distortional buckling strength.

In standard EC3, the design of uniformly compressed elements with either edge or intermediate stiffener assumes that the stiffener behaves as a compressed member with continuous elastic restraint. This restraint has a spring stiffness that depends on the boundary conditions of the

element and on the flexural stiffness of the adjacent plane elements of the cross-section. The elastic critical buckling stress is given by Timoshenko and Gere [8]. The stiffness in the longitudinal direction and the torsional stiffness are both ignored [21–22], as shown in Fig. 3.

Strength assessment in the European standard requires a complex calculation procedure. The distortional buckling is introduced by calculating the reduced thickness of the effective area. The area concerned with this buckling mode is that of the edge stiffener and the adjacent part of the compressed flange. The thickness reduction factor for distortional buckling, χ_d, which is the key parameter defining this instability, depends on the material's yield strength f_{yb}, and also on the elastic buckling stress of the edge stiffener $\sigma_{cr,s}$. It is expressed in terms of the relative slenderness $\overline{\lambda}_d$ as:

if $\overline{\lambda}_d \leq 0.65$ $\quad \chi_d = 1$, $\qquad$ (6)

if $0.65 < \overline{\lambda}_d < 1.38$ $\quad \chi_d = 1.47 - 0.732\overline{\lambda}_d$, $\qquad$ (7)

if $\overline{\lambda}_d \geq 1.38$ $\quad \chi_d = \dfrac{0.66}{\overline{\lambda}_d}$, $\qquad$ (8)

with

$$\overline{\lambda}_d = \sqrt{f_{yb}/\sigma_{cr,s}} \ . \qquad (9)$$

The elastic buckling stress of the edge stiffener is given by:

$$\sigma_{cr,s} = \frac{2\sqrt{KEI_s}}{A_s}, \qquad (10)$$

where A_s and I_s are the effective area and second area moment of the stiffener, respectively; K is the stiffness of the support as stated in EC3.

3 Buckling mode classification of C sections subjected to compression

The buckling mode of simply supported and uniformly compressed lipped channel sections can be identified and characterized by assessing the value of the appropriate plate buckling coefficient, k_v, for each element making up a member [15]. This approach considers the cross-sectional deformation modes, namely (i) the local buckling, involving only the plate transverse bending, and (ii) the distortional buckling, which combines the plate bending with the cross-sectional distortion, and takes into account the interaction between the interconnected plates that form the cross-section.

The plate buckling coefficient k_v values can be found by using the Timoshenko and Gere formula [8] as Eq. (11):

$$k_{vi} = \frac{12\left(1 - v^2\right)}{\pi^2} \frac{\sigma_{cr}^{FSM}}{E} \left(\frac{b_i}{t}\right)^2 . \qquad (11)$$

Where b_i is the width of the plan element forming the section of the member; this element can be the web height, h, the flange width, b, or the lip stiffener, c. Also, t is the thickness of the section, E is Young's modulus, and σ_{cr}^{FSM} is the critical local stress which may be estimated via a Finite Strip Method (FSM) analysis.

The value obtained must be compared with two limits values. These limit values depend on the end conditions of the plate under consideration (i.e., web, flange or edge stiffener), where (i) $k_v = 4$ for a simply supported plate and (ii) $k_v = 0.425$ for a plate with one free edge. The web and flange are stiffened elements; they can therefore be considered as simply supported plates. However, the edge stiffener is an unstiffened element and can be viewed as a plate with one free edge.

The plate buckling coefficient k_v in Eq. (11) can be computed to analyze the buckling behavior of the three elements making up the section (i.e., web, flange and edge stiffener), giving rise to the following four situations that are distinguished by the k_v value:

If $k_v < 0.425$, the instability of the whole section is considered to be far from being triggered by the unstiffened plate local buckling mode.

If $k_v \leq 4$, the local stiffened plate buckling mode does not present the main aspect of the structural behavior of the element.

The last two situations occur when $k_v > 4$ and $k_v > 0.425$. In these two cases, the local buckling of stiffened and unstiffened elements dominates the buckling behavior of the cross-section.

This reasoning makes the identification of the relevant local buckling of lipped channels possible; this can be performed by removing the implausible local instabilities, which certainly correspond to the distortional buckling. Hereafter, a summary of the different situations that occur in the case of symmetric lipped channel columns is given.
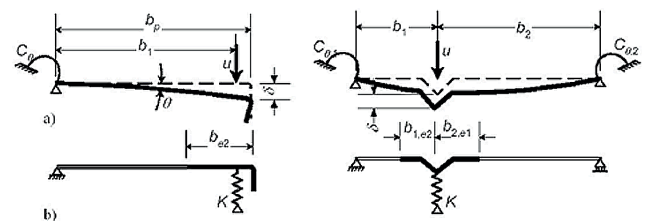

Fig. 3 European standard solution for modeling the distortional instability [25]

The web is a stiffened plane element. The limit to its buckling is thus characterized by a plate buckling coefficient that is equal to 4. The colored part in Fig. 4 is the domain that corresponds to a plate buckling coefficient k_{v1} greater than 4. Outside this domain, the instability of the C-shaped section can in no way be caused by the buckling of the web.

The stiffener, of width c, is an end plate; it is obviously an unstiffened plate. Its buckling cannot be determinative in the instability of a section if k_{v3} is less than 0.425. The border is almost a line that grows very slightly with the size of the flange, as shown in Fig. 5. It can be said that, in general, the stiffener buckling cannot cause the instability of the C-shaped section when the ratio (c/h) is less than 0.3.

As for the flange, we can easily imagine that, depending on the size of the stiffener, its common edge with this stiffener can be considered as either free or supported. Thus, if k_{v2} is less than 0.425, then the flange buckling is excluded. If $0.425 \leq k_{v2} \leq 4$, then the flange buckling with inefficient stiffener is probable; in this case, it is the buckling of the flange as a stiffened plate that is excluded. In the latter case $k_{v2} > 4$, the buckling of the flange with efficient stiffener becomes probable (Fig. 6).

Consequently, the buckling behavior of lipped channel columns can be classified into 8 different instabilities, as can be seen in Fig. 7. Note that the proposed approach was developed by analyzing the buckling behaviors of 364 lipped channel sections. It is worth recalling that the flange width to web height (b/h) considered here is between 0.1 and 1, whereas the lip depth to web height (c/h) values range from 0 to 0.5.

The first Zone (1) corresponds to the local buckling of the web and the second Zone (2) conforms to the instability caused by local buckling of the web and stiffener. On the other hand, the buckling of the web and flange as an unstiffened plate characterize the structural behavior of the sections that belong to the third Zone (3). Moreover, the buckling of the web and/or stiffener as an unstiffened plate
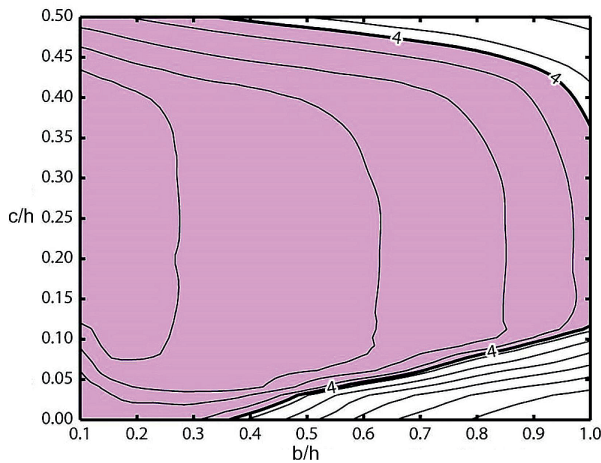

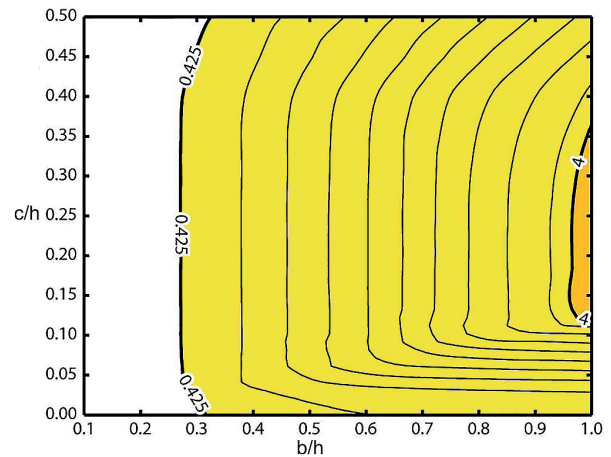**Fig. 4** Probable local buckling zone of the web

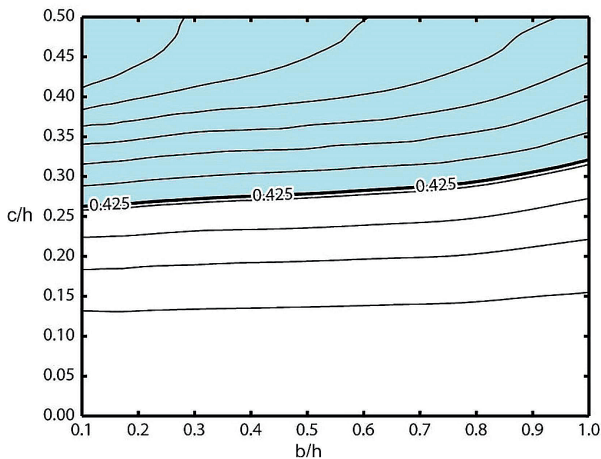**Fig. 6** Probable local buckling zone of the flange

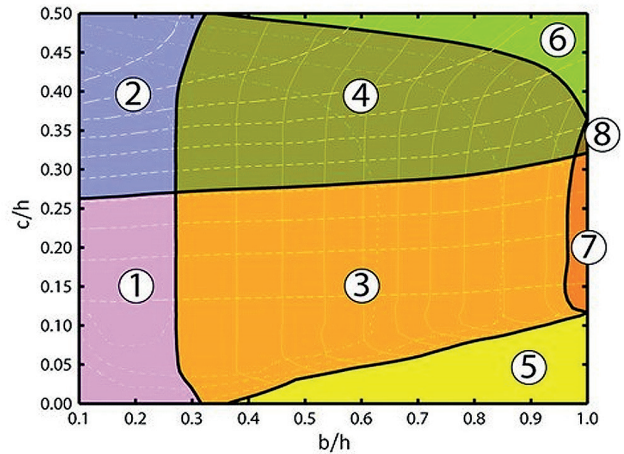**Fig. 5** Probable local buckling zone of the stiffener

Fig. 7 Zones corresponding to different types of instability of C-profiles subjected to compression

refers to Zone (4). The buckling of the insufficiently stiffened flange defines the behavior in Zone (5). As for Zone (6), the instability affects both the flange and the stiffener, but the distortional instability cannot be explicitly noted. This is certainly due to the fact that the stiffener is sufficiently long and its behavior is governed by the local buckling. The seventh Zone (7) is distinguished by the local buckling of the web and that of the flange as a stiffened plate. Finally, the buckling of the stiffener as an unstiffened element, designates the behavior in the eighth Zone (8).

The deformed shape of a compressed lipped channel section of the two buckling classes, namely local and distortional buckling, for each of the foregoing zones, are summarized in Table 1. However, for the zones that did not present a distinct local or distortional minimum, the structural behavior of sections is potentially governed by coupled modes.

In order to consolidate the results of the interesting classification approach for buckling modes, and to highlight the fact that the zoning concept actually governs the structural behavior of cross-sections, a comparative study was carried out in the following section for the purpose of assessing the reliability of the distortional buckling models given in the different design codes for each zone. For this reason, a simplified model that can account for distortional buckling is proposed here according to the classification approach given in Section 3.

4 A design method for elastic distortional buckling stress of lipped channel columns
4.1 Generalities
The classification procedure presented above aims at eliminating the improbable local instabilities which are inevitably distortional instabilities. The present work helps to better understand the complex behavior of cold-formed steel sections; this behavior depends essentially on the section geometry. Moreover, it is irrational to classify instabilities involving the rigid mode displacement of the flange-stiffener set in the distortional mode, regardless of the dimensions of the section. In other words, another type of local buckling mode can lead to this shape deformation. For this reason, the present study aims to provide simplified expressions that help to predict the distortional buckling stress, for which the Timoshenko and Gere theory is applied. A parametric study was therefore conducted on the sections under study in order to promote a better understanding of distortional buckling and their effects, and also to find out the way this mode may be handled in the modern design codes. The development of simplified equations is presented as well.

4.2 A comparative study of design methods for distortional buckling
A number of parametric studies were carried out on the 364 lipped channels [26–27]. The elastic critical loads for different models of distortional buckling modes were compared with the elastic distortional critical loads of the finite strip method (FSM). The cross-sections under consideration cover a relatively wide range of shapes, but only those which satisfy the geometric criteria of the considered codes were taken into consideration. Note that h is the web depth, b is the flange width, c is the lip stiffener length, and t is the material thickness. These dimensions are illustrated in Fig. 8. The applied dimensions are so that:

$0 \leq (c/h) \leq 0.5$
$0.1 \leq (b/h) \leq 1.0$
$0.031 \leq (c/b) \leq 3.27$

Table 1 Modes of instability: local mode and distortional mode corresponding to the 8 zones of instability classification

Zone 1		Zone 2		Zone 3		Zone 4	
	Indistinct Distortional minimum		Indistinct Distortional minimum				Indistinct Distortional minimum
Local	Distortional	Local	Distortional	Local	Distortional	Local	Distortional

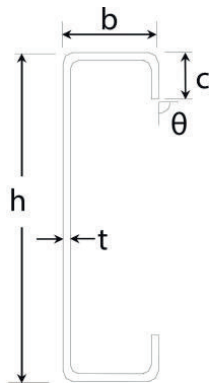| Zone 5		Zone 6		Zone 7		Zone 8	
Indistinct local minimum			Indistinct Distortional minimum				
Local	Distortional	Local	Distortional	Local	Distortional	Local	Distortional

Fig. 8 Dimensions of the C-shaped section

One can easily notice that these are out-to-out dimensions, and all the cross-section elements are perpendicular to each other. Moreover, the cross-sections under study have a thickness t such that $0.48 \le t \le 2.67$ and have rounded corners with a 2 mm internal radius. A regular steel material is assumed to have $E = 210$ Gpa, $v = 0.3$ and $f_y = 320$ MPa.

Furthermore, the critical elastic distortional buckling loads were calculated using (CUFSM) [23], which is a free-to-use package that uses the semi-analytical finite strip method. The distortional critical stresses do not depend on the applied discretization. It is worth noting that the distortional mode may interact with other modes that are highly sensitive to the applied mesh (e. g. local modes). Therefore, the finite strip method calculations may be achieved using 4, 4, 4, 4 strips for each of the lip, flange, web and each one of the corners, respectively; this makes up 35 strips in total, with 36 nodal lines, as illustrated in Fig. 9. The FSM analyses were performed with a single half-wave, which means that the number of degrees of freedom is 144.

On the other hand, it is important to acknowledge that the finite strip method (FSM) has often been unable to provide distinct minima that correspond to distortional
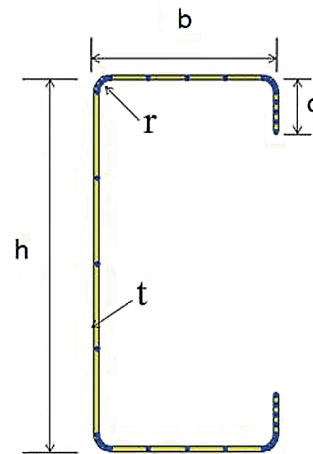

Fig. 9 FSM approach for the rounded-corner model

buckling modes. In fact, a coupled instability phenomenon is naturally included in the conventional finite strip method (FSM) solution, which makes it difficult to determine the relevant distortional buckling modes of members. In the present paper, the "FSM at cFSM buckling length" approach is used [19] in order to avoid the subjec-tive identification process. This approach requires a two-step analysis procedure that may lead to a pure mode solution and an all-mode solution. The pure mode calculation was performed using the constrained Finite Strip Method (cFSM) [6] in order to find the critical buckling half-wavelength L_{crD} which is then applied in a simple finite strip method to determine the elastic buckling load P_{crD}. In addition, it is worth noting that the cFSM pure distortional mode calculation uses a sharp-cornered model, while the conventional FSM analysis employs a model with rounded-corners.

The findings for all 8 zones are depicted in Figs. 10–17, and are summarized in Table 2. A careful observation of these figures and table prompts the following remarks:

Table 2 Performance of the distortional buckling prediction methods

Zone	PcrFSM/PcrEC3			PcrFSM/PcrAISI S100			PcrFSM/PcrAS-NZS		
	Number	average	St. dev	Number	Average	St. dev	Number	Average	St. dev
1	65	0.59	0.17	67	0.94	0.09	30	1.67	1.87
2	/	/	/	30	0.91	0.02	30	1.79	0.24
3	112	1.28	0.32	112	0.97	0.06	112	0.98	0.07
4	19	3.53	1.86	30	0.84	0.05	30	1.23	0.20
5	8	3.59	0.37	30	1.17	0.16	30	1.23	0.20
6	18	1.68	0.35	30	0.87	0.03	30	1.31	0.16
7	35	3.32	1.96	35	0.90	0.03	35	1.13	0.05
8	30	4.38	2.36	30	0.83	0.01	30	1.14	0.07
Total	287	2.62	1.05	364	0.92	0.05	327	1.31	0.35

- The American model gives the best results, which can clearly be observed through the weak dispersion of the majority of zones.
- The American model exhibits equivalent results in zones four (Fig. 13), six and eight (Figs. 15 and 17); all results are grouped around the Value 1. In these instances, the critical load remains relatively larger than the one obtained with the finite strip method.
- The American model (NAS/AISI S100, 2007) presents the largest standard deviation for zone one, and zone five, with values 0.09 and 0.16, respectively; they are clearly illustrated. However, the best performance for this model is confirmed in all the other zones.
- The American and Australian models display the same performances in the third and fifth zones (Figs. 12 and 14), as well as in the seventh and eight zones (Figs. 16 and 17); however, different behaviors are observed in Zones 1, 2, 4, 6.
- It was found that the Australian model for zone three (Fig. 12), zones seven and eight (Figs. 16 and 17) give the best standard deviation values, equal to 0.07, 0.05 and 0.07, respectively.
- Figs. 10 and 11 suggest that for some sections in Zone 1 and Zone 2, the results obtained with the Australian method are not strongly consistent with those of the finite strip method.
- The European model shows a good congruence with the numerical results, but only for some configurations of the third zone (Fig. 12) and first zone (Fig. 10), which indicates that the EC3 model may be adapted only in this interval of geometries in order to represent the distortional mode. The configurations in these sections are characterized by wide flanges and relatively small stiffeners. Furthermore, the sections in Zone 2 (Fig. 11), and some other zones, i.e. 4, 5, and 6 (Figs. 13–15), did not give any results. The model developed by Eurocode for the distortional mode may not accurately represent the actual structural behavior of these sections during the elastic stability of the structural elements. The structural behavior may be governed by the local buckling or by a coupled mode for the considered dimensions.

Based on the findings of this work, the following conclusions can be drawn:

Depending on the dimensions of the section, each type of behavior can be modulated either in an individual behavior (local buckling), or in a global behavior (distortional buckling) of the flange-stiffener subset; it may eventually be modulated in a combined behavior. In other words, it is possible to develop a novel approach that can handle the distortional buckling based on local buckling of the plate elements making up the section.

The American model and the Australian model, are based on the flexural-torsional buckling of the stiffened flange; however, the web undergoes a plate-like flexural deformation. Moreover, the suggested approach implies that the local buckling of the web leads to this mechanism. In other words, the evolution of the web local instability causes the rotation of the flange-stiffener subset. However, the most plausible explanation, when considering the European model, is that the local mode of slender flanges may lead to the flexural buckling of the stiffener and the adjacent portion of the flange. Therefore, this approach could be useful for showing the slight difference between the two approaches indicated in the Design Codes, i.e. AISI/NAS S100 (2007), AS/NZS 4600 (2005) and CEN/EC3, 1993-1-3 (2006). This allows dividing the distortional mode into two types of behaviors. The synthesis of these results makes it possible to conclude that another mechanism for the distortional mode can be highlighted. It is defined by an evolutionary change in the structural behavior, and is then manifested by a switch from the local mode of a low-stiffness plate to a global mode of a subset of plates with significant stiffness.

4.3 A simplified expression for the elastic distortional buckling
4.3.1 Generalities
The distortional mechanism is not unique; it depends on the dimensions of the built-up plate elements (stiffener, flange, and web).

The structural behavior switches from the local buckling of the flange or web to the global buckling of the flange-stiffener subset which is elastically supported by the web. As stated in Section 4.2, the American model is not sufficiently efficient to represent the real behavior of the cross-sections in Zones 1 and 5. The behavior of sections in Zone 1 is evidenced by the local buckling of the web; this behavior causes the flange-stiffener subset to rotate. However, in Zone 5, the flange local buckling induces a global buckling of the flange-stiffener subset that is elastically supported by the web. Though the deformed shape of the sections belonging to these zones materializes the distortional buckling, the buckling behavior is governed by the local buckling.
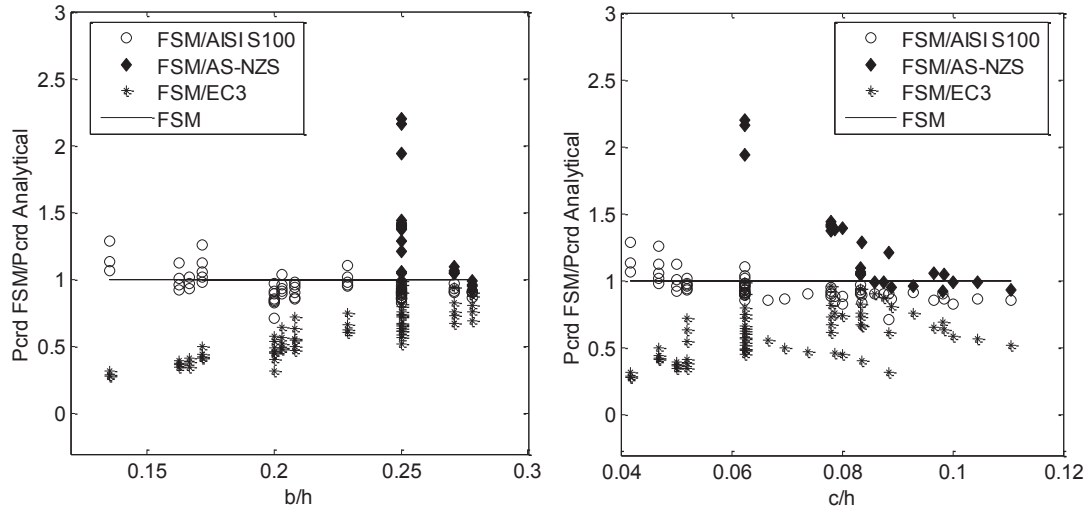
Fig. 10 Comparison of existing analytical models using the numerical results for the first zone sections
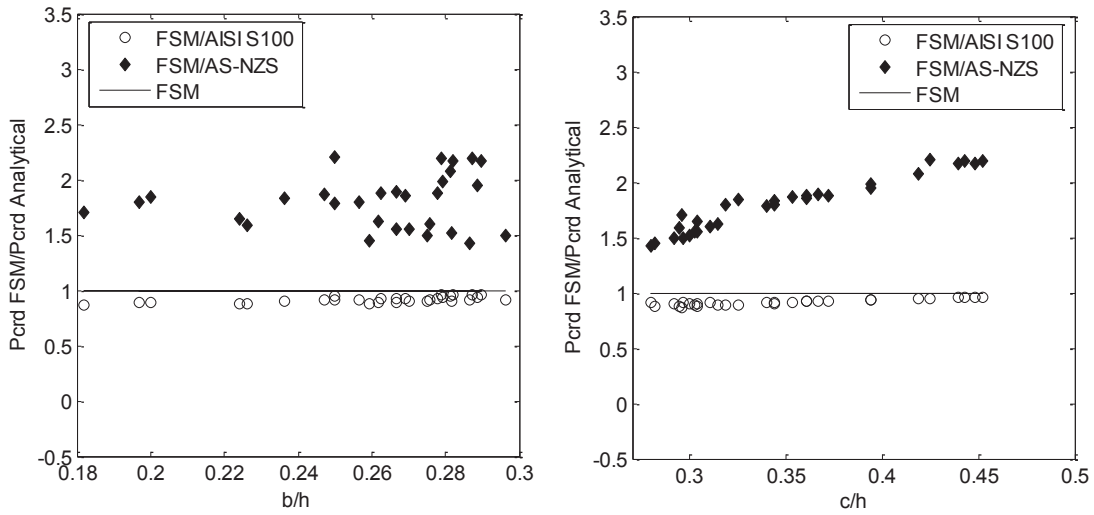

Fig. 11 Comparison of existing analytical models using the numerical results for the second zone sectionsv
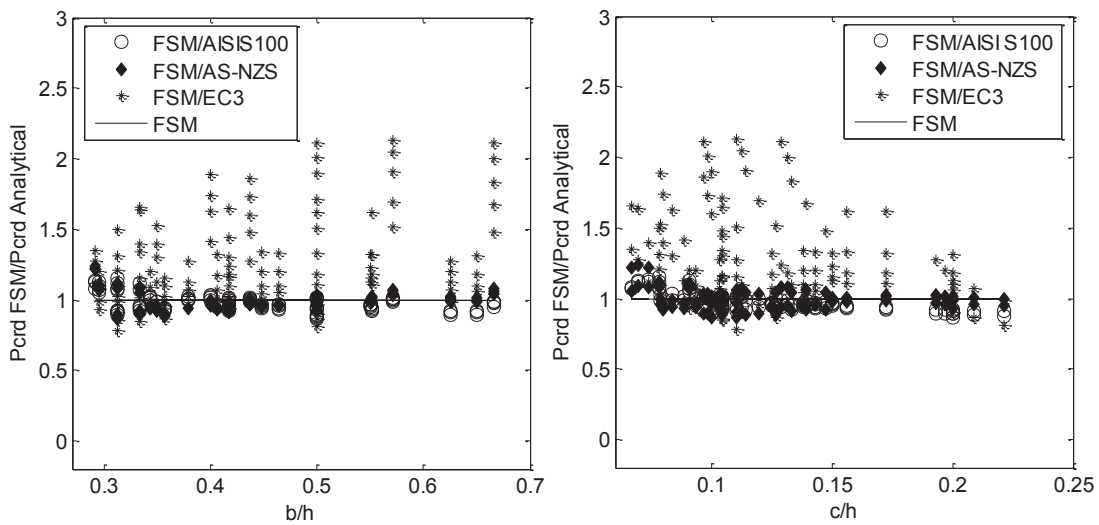

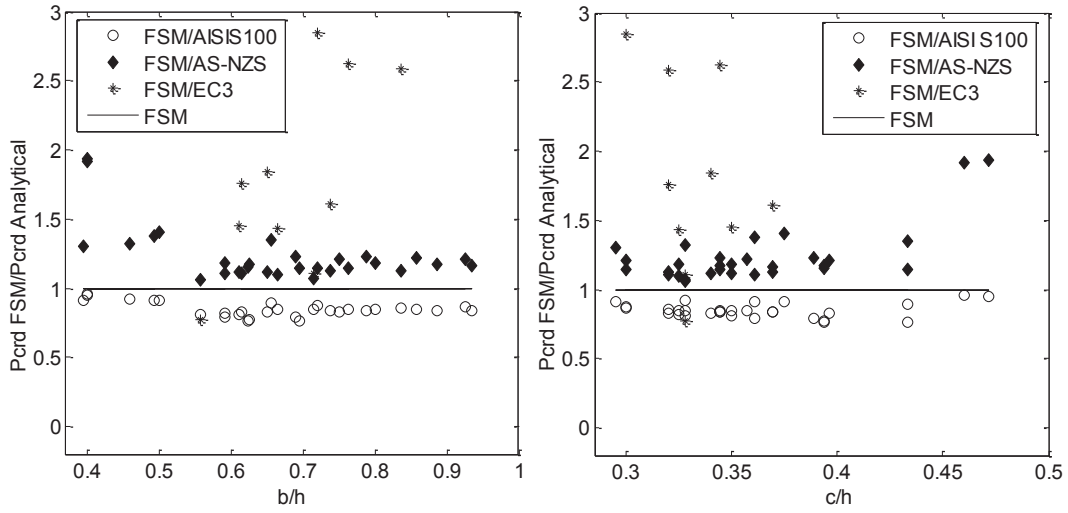**Fig. 12** Comparison of existing analytical models using the numerical results for the third zone sections

Fig. 13 Comparison of existing analytical models using the numerical results for the fourth zone sections
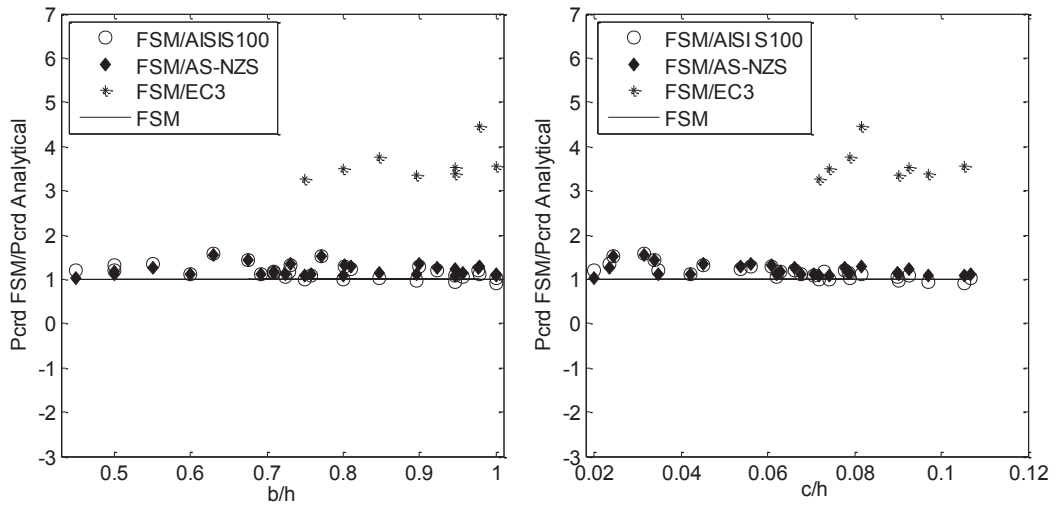

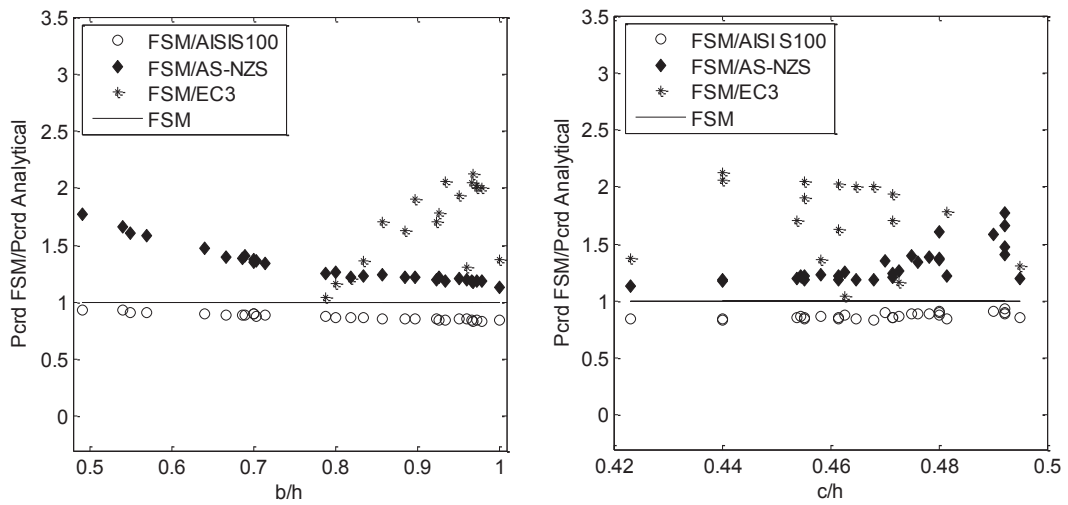**Fig. 14** Comparison of existing analytical models using the numerical results for the fifth zone sections

Fig. 15 Comparison of existing analytical models using the numerical results for the sixth zone sections
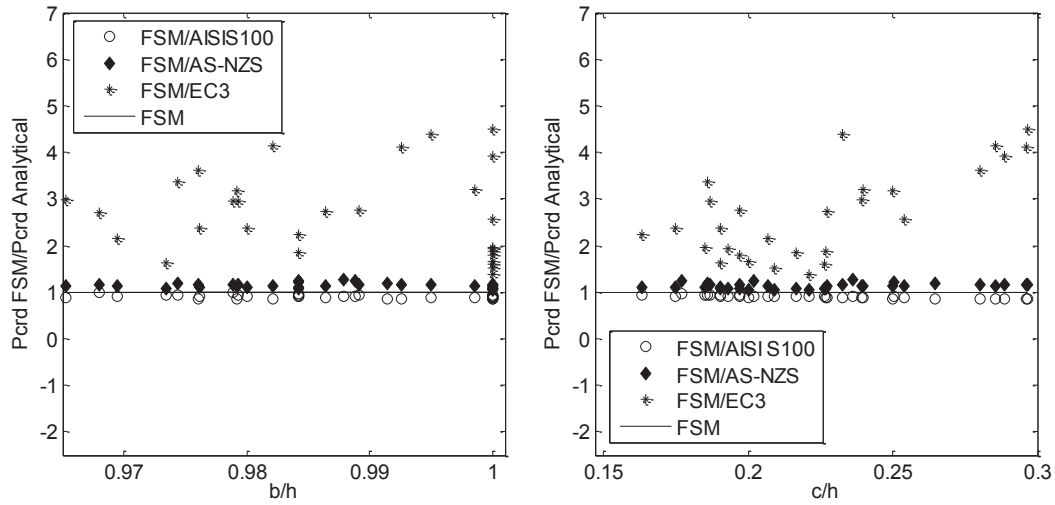
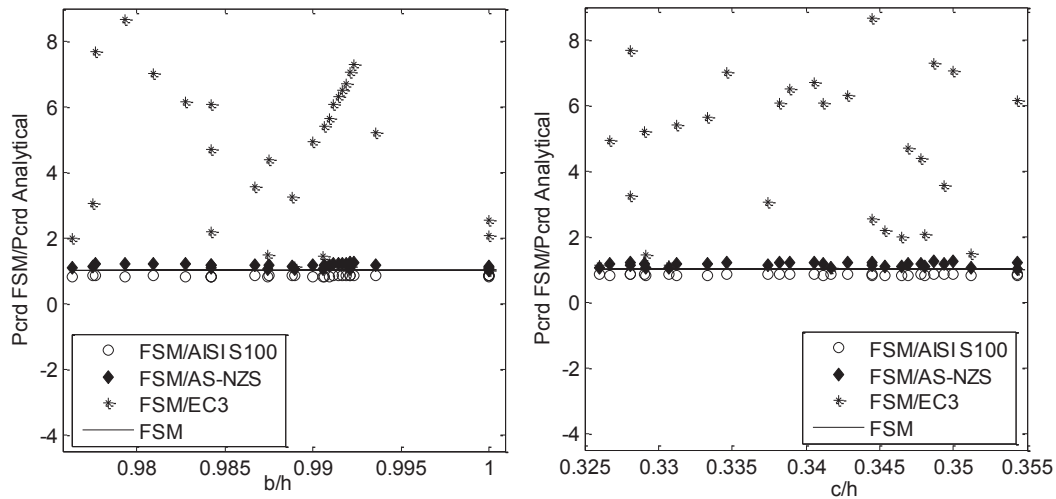**Fig. 16** Comparison of existing analytical models using the numerical results for the seventh zone sections

Fig. 17 Comparison of existing analytical models using the numerical results for the eighth zone sections

4.3.2 Distortional buckling coefficient for Zone 1

The structural behavior in the first zone is governed by the local buckling of the web. The behavior of the web can be described using Timoshenko's theory in which:

$$\sigma_{cr} = k_d \frac{\pi^2 E}{12\left(1-v^2\right)} \left(\frac{t}{h}\right)^2. \tag{12}$$

The expression of the plate buckling coefficient for distortional buckling k_d Eq. (13) is derived from a statistical procedure that is founded on a multiple linear regression model for a relatively wide range of cross-sectional dimensions. Fig. 18 indicates that this formulation gives better results with respect to the numerical results.

$$k_d = 20.433\left(\frac{b}{h}\right) + 0.782\left(\frac{c}{t}\right) - 2.351. \tag{13}$$

The average ratio of the distortional critical stress from the finite strip method (FSM) to that resulting from the proposed method is 1.004, with a standard deviation equal to 0.061 for all 67 sections of Zone 1.

In order to assess the applicability of the proposed formulation, 30 cross-sections were used for the calculation of elastic distortional buckling loads of members subjected to compression using the proposed model. The obtained results were compared with those found with the finite strip method (FSM). It was found that the proposed model systematically predicted distortional buckling stress results that are close to those obtained by the finite strip method, for all 30 cross-sections, with an average value of 0.96 and a standard deviation of 0.04.
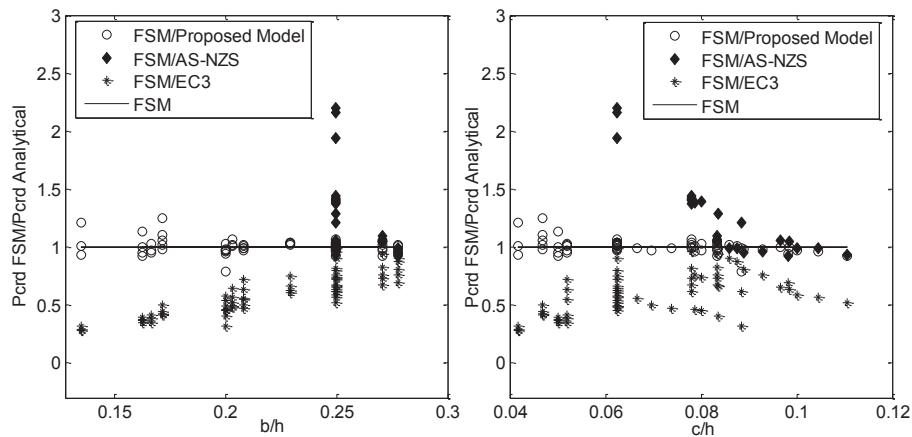
Fig. 18 Performance of the proposed model for sections of the first zone

Moreover, the proposed formula for the plate buck-ling coefficient k_d of the web Eq. (13) is more linear than Eq. (15) which is provided by the AISI S100 method. It helps to improve the quality of the results, and therefore reduces the number of scattered results.

$$F_d = \alpha k_d \frac{\pi^2 E}{12(1-v^2)} \left(\frac{t}{b}\right)^2, \tag{14}$$

$$k_d = 0.05 \leq 0.1 \left(\frac{bcsin\theta}{ht}\right)^{1.4} \leq 8. \tag{15}$$

Where α is a value that accounts for the advantage of an unbraced length L_m which is shorter than L_{cr}, but can con-servatively be taken equal to 1; θ is the lip angle.

The AISI S100 model for the range of geometries of sections in Zone 1 is governed by Eq. (14) [16] proce-dure (a) of Chapter C, Section C 4.2 which assumes that the flange local buckling controls the behavior of the sections. However, this design model gives an average value of 1.76 and a standard deviation of 0.50, as depicted in Fig. 19.
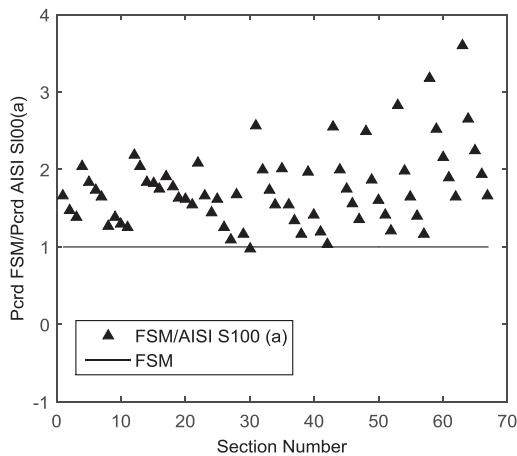

Fig. 19 Comparison of the AISI S100 model results with those given by the finite strip method, for Zone 1

It is interesting to note that the classification approach proves that the web local buckling is the main behavioral aspect of sections in Zone 1. Note that the new formula-tion Eqs. (12–13) was developed in accordance with this approach. The new model is direct, simple, and linear; it can predict the distortional buckling stresses that are found closer to the numerical results.

The proposed model is based on selected cold-formed steel sections. The following geometric limitations should be considered, when this new approach is applied:

The proposed model	*AISI/NAS S100, 2007*
$50 \leq h/t \leq 384.60$	$50 \leq h/t \leq 200$
$13.5 \leq b/t \leq 98.33$	$25 \leq b/t \leq 100$
$3.68 \leq c/t \leq 35$	$6.25 \leq c/t \leq 50$
$0.2 \leq b/h \leq 0.28$	$0.125 \leq b/h \leq 0.5$
$0.04 \leq c/h \leq 0.11$	$0.005 \leq c/h \leq 0.25$
$0.16 \leq c/b \leq 1$	$0.04 \leq c/b \leq 0.5$

It seems that the range of validity of the proposed model is almost equivalent to that of the American model.

4.3.3 Distortional buckling coefficient for Zone 5

The flange local buckling is the behavior that characterizes the fifth zone sections, as previously mentioned. Theses sec-tions are characterized by wide flanges and small stiffeners, also called insufficiently stiffened flanges. It is important to note that the sections buckle in the local buckling mode.

The plate buckling coefficient for distortional buck-ling k_d, which takes into account the interaction between the elements making up the section and allows an accu-rate estimation of the elastic distortional buckling stress, is given by Eq. (16) and depicted in Fig. 20. The following equation can therefore be obtained from a statistical analy-sis that is based on a simple linear regression model.

$$\sigma_{cr} = k_d \frac{\pi^2 E}{12(1-v^2)} \left(\frac{t}{b}\right)^2 \quad k_d = 0.3038\left(\frac{bc}{ht}\right) + 0.8011 \,. \quad (16)$$

In order to check the validity of the proposed model, an analysis was performed on 31 cross-sections to estimate the elastic distortional buckling stress which is expressed by Eq. (16). The results obtained were found compatible with those of the finite strip method for all the specimens. The average turned out to be equal to 0.99 with a standard deviation of 0.10.

The use of the proposed formulation allows a straightforward, accurate and linear prediction of the elastic distortional buckling stress.

The geometric limitations for Zone 5 are compared with those of AISI/NAS S100 (2007) as follows:

The proposed model	AISI/NAS S100, 2007
$0.4 \le b/h \le 1$	$0.125 \le b/h \le 0.5$
$0.03 \le c/b \le 0.12$	$0.04 \le c/b \le 0.5$
$0.05 \le c/h \le 0.10$	$0.005 \le c/h \le 0.25$

The interval of validity of the proposed model is close to that of the AISI S100 model.

5 Conclusions
It is frequently assumed that the buckling mode plays a predominant role in the behavior of cold-formed steel structures and the ultimate strength of structural elements. It is widely accepted today that the analytical approaches are sufficiently available; besides, the developed numerical methods are currently much more efficient and accurate for analyzing the behavior of thin-walled members.

This paper provides a review of design codes relating to the distortional strength of simply supported lipped channel sections subjected to compression. Additionally, a comparative study based on different code provisions was also conducted, and the resulting findings were compared with the respective numerical results. Globally, this study allows drawing some interesting conclusions, as listed below:

(i) The buckling mode of lipped channel sections can be determined through an identification process using the plate buckling coefficient which takes into account the interactions between the various elements making up the section.

(ii) The behavior of the first zone is characterized by the local web buckling which consequently leads to the rotation of the flange-stiffener subset with respect to the web-flange junction. Thus, in the fifth zone, the flange local buckling causes the longitudinal displacement of the flange-stiffener set, or the stiffener and the adjacent part of the flange.

(iii) The proposed expressions help engineers to design the distortional buckling of cold-formed steel structural elements, with a simple, linear and straightforward procedure.

(iv) The proposed expressions were calibrated to the finite strip method; they showed a better performance than that of the AISI S100 method.

In the end, it is worth noting that further research on methods for the prediction of distortional modes, which are based on the earlier classification approach and correspond to other geometric configurations and loading types, is needed and must be considered in future studies.
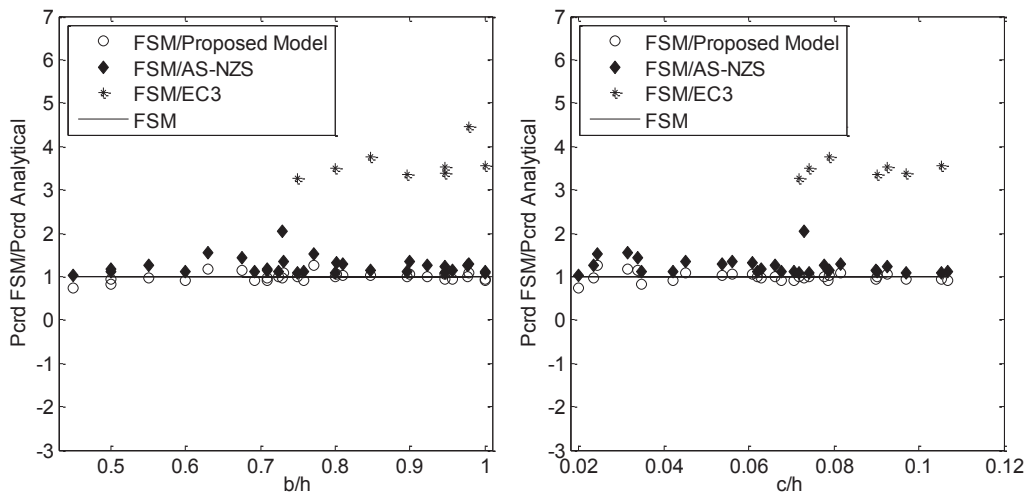
Fig. 20 Performance of the proposed model for the fifth zone

References

[1] Yu, C., Yan, W. "Effective Width Method for determining distortional buckling strength of cold-formed steel flexural C and Z sections", Thin-Walled Structures, 49(2), pp. 233–238, 2011.
https://doi.org/10.1016/j.tws.2010.11.006

[2] Silvestre, N., Camotim, D., Dinis, P. B. "Post-buckling behaviour and direct strength design of lipped channel columns experiencing local/distortional interaction", Journal of Constructional Steel Research, 73, pp. 12–30, 2012.
https://doi.org/10.1016/j.jcsr.2012.01.005

[3] Bešević, M., Prokić, A., Landović, A., Kasaš, K. "The Analysis of Bearing Capacity of Axially Compressed Cold Formed Steel Members", Periodica Polytechnica Civil Engineering, 61(1), pp. 88–97, 2017.
https://doi.org/10.3311/PPci.8836

[4] Casafont, M., Marimon, F., Pastor, M. M. "Calculation of pure distortional elastic buckling loads of members subjected to compression via the finite element method", Thin-Walled Structures, 47(6–7), pp. 701–729, 2009.
https://doi.org/10.1016/j.tws.2008.12.001

[5] Joó, A. L., Ádány, S. "FEM-based approach for the stability design of thin-walled members by using cFSM base functions", Periodica Polytechnica Civil Engineering, 53(2), pp. 61–74, 2009.
https://doi.org/10.3311/pp.ci.2009-2.02

[6] Djafour, M., Djafour, N., Megnounif, A., Kerdal, D. E. "A constrained finite strip method for open and closed cross-section members", Thin-Walled Structures, 48(12) pp. 955–965, 2010.
https://doi.org/10.1016/j.tws.2010.07.004

[7] Djafour, N., Djafour, M., Megnounif, A., Matallah, M., Zendagui, D. "A constrained finite strip method for prismatic members with branches and/or closed parts", Thin-Walled Structures, 61, pp. 42–48, 2012.
https://doi.org/10.1016/j.tws.2012.04.020

[8] Timoshenko, S. P., Gere, J. "Theory of Elastic Stability", Wiley, London, UK, 1973.

[9] Ajeesh, S. S., Arul Jayachandran, S. "Simplified semi-analytical model for elastic distortional buckling prediction of cold-formed steel flexural members", Thin-Walled Structures, 106, pp. 420–427, 2016.
https://doi.org/10.1016/j.tws.2016.05.015

[10] Lau, S. C. W., Hancock, G. J. "Distortional Buckling Formulas for Channel Columns", Journal of Structural Engineering, 113(5), pp. 1063–1078, 1987.
https://doi.org/10.1061/(ASCE)0733-9445(1987)113:5(1063)

[11] Teng, J. G., Yao, J., Zhao, Y. "Distortional buckling of channel beam-columns", Thin-Walled Structures, 41(7), pp. 595–617, 2003.
https://doi.org/10.1016/S0263-8231(03)00007-7

[12] Hancock, G. J. "169.Design for distortional buckling of flexural members", Thin-Walled Structures, 27(1), pp. 3–12, 1997.
https://doi.org/10.1016/0263-8231(96)00020-1

[13] Schafer, B. W., Peköz, T. "Laterally Braced Cold-Formed Steel Flexural Members with Edge Stiffened Flanges", Journal of Structural Engineering, 125(2), pp. 118–127, 1999.
https://doi.org/10.1061/(ASCE)0733-9445(1999)125:2(118)

[14] He, Z., Zhou, X. "Strength design curves and an effective width formula for cold-formed steel columns with distortional buckling", Thin-Walled Structures, 79, pp. 62–70, 2014.
https://doi.org/10.1016/j.tws.2014.02.004

[15] Djafour, M. "Étude de la Stabilité Distorsionnelle des Profils en Acier Formés à Froid (Study of the Distortional Stability of Cold-formed Steel Profiles)", Ph.D Thesis, University of Abou Bekr Belkaïd, Algeria, 2007. (in French)

[16] AISI "AISI S100-07 North American Specification for the Design of Cold-Formed Steel Structural Members", American Iron and Steel Institute, Washington, DC, USA, 2007.

[17] AS/NZS "AS/NZS 4600:2018 Cold-formed steel structures", Standards of Australia and Standards of New Zealand, Sydney, Australia and Wellington, New Zealand, 2005.

[18] CEN "EN 1993-1-3 Eurocode 3 - Design of steel structures - Part 1–3: General rules - Supplementary rules for cold-formed members and sheeting", European Committee for Standardization, Brussels, Belgium, 2006.

[19] Li, Z., Schafer, B. W. "Application of the finite strip method in cold-formed steel member design", Journal of Constructional Steel Research, 66(8–9), pp. 971–980, 2010.
https://doi.org/10.1016/j.jcsr.2010.04.001

[20] Imene, M., Naoual, D., Mustapha, D. "Study of Local and Distortional Stability of Thin-Walled Structuresures", MATEC Web of Conferences, 149, Article ID: 01089, 2018.
https://doi.org/10.1051/matecconf/201814901089

[21] Kesti, J., Davies, J. M. "Local and distortional buckling of thin-walled short columns", Thin-Walled Structures, 34(2), pp. 115–134, 1999.
https://doi.org/10.1016/S0263-8231(99)00003-8

[22] Schafer, B. W., Peköz, T. "The behavior and design of longitudinally stiffened thin-walled compression elements", Thin-Walled Structures, 27(1), pp. 65–78, 1997.
https://doi.org/10.1016/0263-8231(96)00016-X

[23] Thin-Walled Structures "CUFSM 5 - Finite Strip Elastic Buckling Analysis Application", [online] Available at: http://www.ce.jhu.edu/bschafer/cufsm [Accessed: 10 August 2019]

[24] Pala, M. "Genetic programming-based formulation for distortional buckling stress of cold-formed steel members", Journal of Constructional Steel Research, 64(12), pp. 1495–1504, 2008.
https://doi.org/10.1016/j.jcsr.2008.01.018

[25] Ma, W., Becque, J., Hajirasouliha, I., Ye, J. "Cross-sectional optimization of cold-formed steel channels to Eurocode 3", Engineering Structures, 101, pp. 641–651, 2015.
https://doi.org/10.1016/j.engstruct.2015.07.051

[26] American Iron and Steel Institute "AISI Manual Cold-Formed Steel Design 2002 Edition", American Iron and Steel Institute, Washington, DC, USA, Rep. 9-2003, 2003. [online] Available at: http://scholarsmine.mst.edu/ccfss-aisi-spec/130 [Accessed: 10 August 2019]

[27] SSMA "Product Technical Information ICBO ER-4943P", Steel Stud Manufacturers Association, Chicago, IL, USA, 2001, [online] Available at: http://bechtel.colorado.edu/~willam/4830%20SSMA%20Product%20Technical%20Information.pdf [Accessed: 15 December 2011]